INL/CON-24-76284-Revision-0

Design by analysis rules for ASME Section III, Division 5, Class B components

July 2024

Heramb Prakash Mahajan, Robert Jetter, Ting-Leung Sham, Yanli Wang

Changing the World's Energy Future

Idaho National Laboratory

INL is a U.S. Department of Energy National Laboratory operated by Battelle Energy Alliance, LLC

INL/CON-24-76284-Revision-0

Design by analysis rules for ASME Section III, Division 5, Class B components

Heramb Prakash Mahajan, Robert Jetter, Ting-Leung Sham, Yanli Wang

July 2024

Idaho National Laboratory
Idaho Falls, Idaho 83415

http://www.inl.gov

Prepared for the
U.S. Department of Energy
Under DOE Idaho Operations Office
Contract DE-AC07-05ID14517

Proceedings of the ASME 2024
Pressure Vessels & Piping Conference
PVP2024
July 28-August 2, 2024, Bellevue, Washington

PVP2024-122300

DESIGN-BY-ANALYSIS RULES FOR ASME SECTION III, DIVISION 5, CLASS B COMPONENTS

Heramb Mahajan
Idaho National Laboratory
Idaho Falls, ID

Robert Jetter
R. I. Jetter Consulting, CA

Ting-Leung Sham
Idaho National Laboratory
Idaho Falls, ID

Yanli Wang
Oak Ridge National Laboratory
Oak Ridge, TN

ABSTRACT

The current rules for elevated temperature ASME Section III, Division 5, Class B components, other than piping, were basically adapted from the Design-by-Rule approach for Section VIII, Division 1 vessels. A goal of the proposed new rules is to explicitly account for the design life and cyclic service while recognizing the less-rigorous requirements commensurate with lesser safety consideration. Further goals are to maximize the use of modern computational technology, for example finite element analysis in conjunction with reference stress concepts, and to avoid the need for stress classification. This paper summarizes the work done to address these issues. A summary of the design-by-analysis for primary loads, strain limit evaluation, and creep-fatigue damage assessment is presented. The proposed design-by-analysis creep-fatigue damage calculation approach uses a new elastic follow-up-based Isochronous Stress Strain Curve stress relaxation procedure. A set of sample problems are selected to validate the proposed design-by-analysis rules for creep-fatigue damage assessment. The proposed Class B rules are evaluated against the Class A elastic design rules and the experimental data obtained from a family of a simplified model test-based key-feature test results. The proposed Class B creep-fatigue damage assessment methodology yields conservative design cycles estimates compared to the experimental results.

Keywords: Elastic follow-up, Creep-fatigue, Class B rules

NOMENCLATURE

T	Temperature
t	Time
Δt	Time increment
P	Pressure
q	Elastic follow-up
D_c	Creep damage fraction
D_f	Fatigue damage fraction
dD_c	Creep damage fraction in one cycle
dD_f	Fatigue damage fraction in one cycle
S_{LB}	Lower bound stress
N_{max}	Maximum allowable design cycle
N_f	Failure cycles from experiment
$\Delta\varepsilon$	Strain ranges from experiment
ε_t	Enhanced strain range at the end of time t

1. INTRODUCTION

The current rules for elevated temperature ASME Section III, Division 5, Class B components, other than piping, were basically adapted from the Design-by-Rule approach for Section VIII, Division 1 vessels [1]. As such, they explicitly do not consider the effects of cyclic loading. Further, the allowable stress values at elevated temperature where creep effects are significant are based on time-dependent properties at 100,000 hr and not the required service life of the component. The rules for Class B components currently provide for invoking alternative methods for demonstrating compliance relating to buckling, ratcheting, and creep-fatigue failure. However, these alternative methods must be approved by the owner and incorporated into the Design Specifications. The proposed code case will provide an approved methodology.

A goal of the proposed new rules is to explicitly account for the design life and cyclic service while recognizing the less rigorous requirements commensurate with lesser safety consideration. Further goals are to maximize the use of modern computational technology, for example, finite element analysis in conjunction with reference stress concepts, and to avoid the need for stress classification. This paper summarizes the work done to address these issues. A summary of the design-by-analysis for primary loads, strain limit/ratcheting evaluation, and creep-fatigue damage assessment is presented. The proposed load-controlled design limits are based in part on limit load concepts approved for use for Class A components using time-dependent allowable stress values based on the specified service life. Similarly, strain/ratcheting limits are based on part of the strain limits methodology using Elastic Perfectly Plastic (EPP) material modeling approved for Class A components. The

proposed design-by-analysis creep-fatigue damage calculation approach uses a new elastic follow-up-based Isochronous Stress Strain Curves (ISSCs) stress relaxation procedure. A set of sample problems are selected to validate the proposed design-by-analysis rules for creep-fatigue damage assessment. The proposed Class B rules are evaluated against the Class A elastic design rules and the experimental data obtained from a family of a simplified model test-based key-feature test results. The proposed Class B creep-fatigue damage assessment methodology yields conservative design cycles estimates compared to the experimental results.

2. PROPOSED CLASS B RULES

The proposed new rules for Class B are described in more detail below. Because the focus of this paper is on the new rules for evaluation of creep-fatigue damage, the rules for primary loading and ratcheting are described in general terms and more specific information is provided for creep-fatigue.

2.1 Primary Load

As noted above, there are two main goals of the proposed evaluation procedures for load-controlled stresses. The first is to explicitly account for long term specified design life and the second is to avoid the need for stress classification. A companion issue to the above is the definition of allowable stress criteria for extended time-dependent service lives. Also, as noted above, the current rules rely on the allowable stress values tabulated in Section II of the ASME B&PV Code that are based on extrapolated creep properties at 100,000 hr that do not explicitly address deign margins for extended operating hours such as 300,000 hr design life [2].

A design evaluation methodology based on Code Case N-924 for Class A components provides a framework for the proposed rules for Class B. As in the current rules for Class B, Design Conditions are evaluated using allowable stress values from Section II. However, to avoid stress classification in the proposed Class B methodology, the allowable load is based either on the design-by-rule procedures in NCD-3300, -3400, and -3500, or on the limit load, EPP-based (DBA) procedures in CC N-924. For Service Loadings, which would include extended service lives, the allowable load is similarly based on the DBA procedures in CC N-924. However, the allowable stress values in the proposed Class B are not as tabulated in Section II. The proposed approach is to base the allowable stress values in the Class B code case on the specified design life, t_D, at temperature instead of 100,000 hr. The variable design lifetime procedure discussed in the previous report [3] was used. This calculation procedure provided the time-dependent allowable stress in the creep regime for the target design life, t_D.

These new values are applicable to Service Loadings not Design Conditions. As a result, at 100,000 hr the required thickness would be governed by the standard Section II values as Service Loadings are nominally somewhat less than Design Conditions. However, for a longer specified design life, the required thickness would be governed by the new Service Loading stress values. Also, note these criteria for Class B are not as conservative as the criteria for Class A (e.g., 67% of the stress to rupture in the specified life for Class A versus 80% of the similar stress to rupture for the proposed new Class B values).

A further advantage of the proposed approach to allowable stress values is that it is based on the same creep parameters used for Section II, Table 1 and thus, hopefully, there will be data available for more materials than the limited number included for Class A at elevated temperature.

2.2 Ratcheting Check

Code case N-861-2 provides a methodology for satisfying strain limits for elevated temperature Class A components. As part of those requirements, shakedown or freedom from ratcheting must be demonstrated as well as specific strain limits. For Class B, satisfaction of specific strain limits is not required but shakedown and freedom from ratcheting is required. The evaluation methodology is based on an EPP material model with a pseudo yield strength, where the pseudo yield strength in the creep regime is defined as the stress from the applicable ISSCs for the temperature of operation that yields a strain of 1% for base metal and 0.5% for weldments. The rationale for this abbreviated approach is that strain accumulation within bounds is not directly related to failure and a pseudo yield strength of 1% provides an adequate bound for Class B components. Further, use of the EPP material model and absence of ratchetings avoids the need for stress classification.

2.3 Creep-Fatigue Damage Assessment

As noted, the proposed approach for assessment of creep-fatigue damage is new. However, the basic concepts have been employed in various forms. The basic approach is the same as that from Class A wherein the calculated fatigue damage is the familiar summation of the number of applied cycles of a specific magnitude divided by the allowable number of cycles of that magnitude, $\left(\frac{n}{N_d}\right)$, and the creep damage is the summation of actual time duration at an incremental stress level divided by the allowable time duration at that stress level to avoid creep rupture, $\left(\frac{\Delta t}{T_d}\right)$. The interaction of fatigue and creep damage is accounted for with an allowable combined damage, D, as shown in Figure 1.

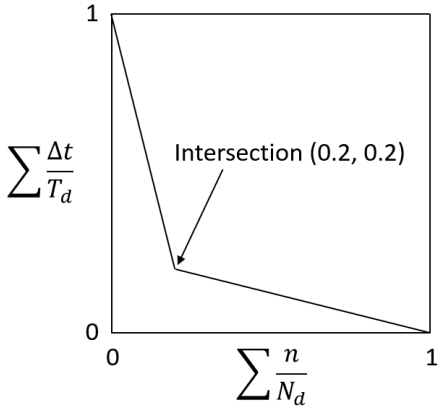

FIGURE 1: Creep-fatigue damage envelope.

Based on consideration of creep-fatigue interaction and the impact on design allowable cycles, a damage intercept of (0.2, 0.2) was considered to be a sufficiently conservative approximation for use with the design methodologies applicable to the less rigorous safety considerations applicable to Class B.

2.3.1 Creep-Fatigue Evaluation Methodology

The methodology used to evaluate the enhanced strain range and creep damage during cyclic service is based on the use of ISSCs to determine stress and strain histories where the component configuration is such that there are elastic follow-up effects to be considered. The concept is illustrated by Figure 2.

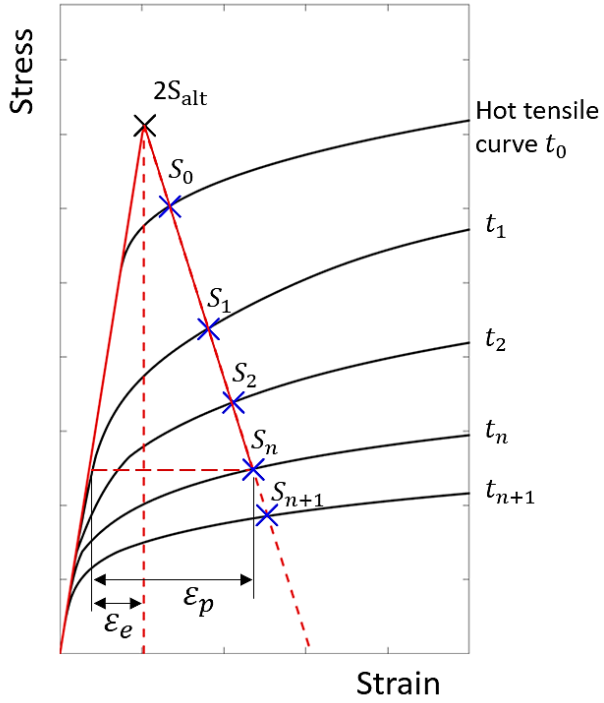

FIGURE 2: Stress and strain history using isochronous stress-strain curve relaxation intercepts.

In this case, the elastically calculated peak stress is determined in accordance with the methodology defined in Section III, Appendix XIII-3520(e) using the stress difference procedure described in XIII-2400. The follow-up factor, $q = \frac{\varepsilon_p}{\varepsilon_e}$ is a function of component geometry and can be determined by inelastic analysis. However, for structures without sharp stress concentrations, or unbalanced piping systems, $q = 3$ is a reasonable upper bound and $q = 2$ is a conservative representative value [4].

The creep damage for each cycle type can be calculated incrementally from the expression:

$$\sum_{n=1}^{n} \frac{t_n - t_{n-1}}{(T_d)_n} = D_{cj} \qquad (1)$$

$(T_d)_n$ = allowable time duration determined from stress-to-rupture curves for a given stress and the maximum temperature at the point of interest and occurring during the time interval, $(t_{n+1} - t_n)$. However, the stress relaxation is limited by a lower bound stress relaxation, S_{LB}, due to the presence of primary load effects that do not relax out. This is shown conceptually in Figure 3.

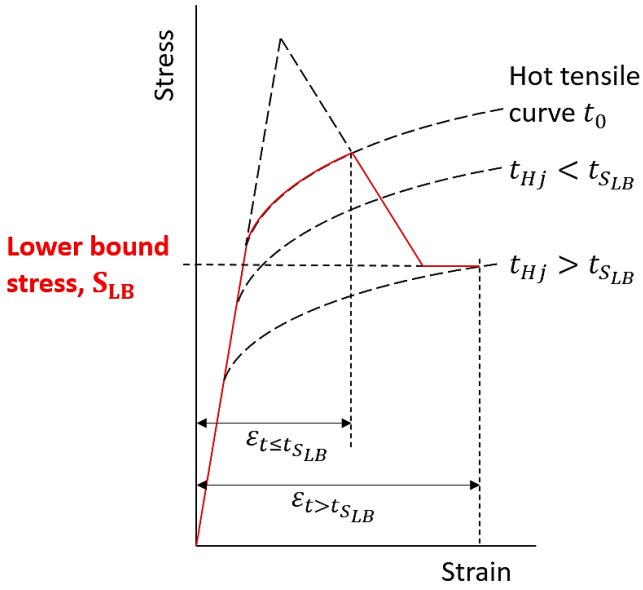

FIGURE 3: Stress relaxation limited by lower bound stress.

If the stress has not relaxed below S_{LB} during the reference hold time, t_h, then the strain range is given by $\varepsilon_{t<t_{LB}}$. If the lower bound stress limits the stress relaxation, then the strain range is given by $\varepsilon_{t>t_{LB}}$. The value of S_{LB} may be determined from the limit load calculations in the primary stress evaluation.

3. EVALUATION OF THE PROPOSED CLASS B DESIGN-BY-ANALYSIS RULES

The previous section provides a general description of the proposed Class B DBA rules. Figure 4 shows the stepwise creep-fatigue damage assessment approach adopted in this study. The first step was to conduct an elastic transient finite element analysis with all geometric details. This analysis includes pressure and spatial temperature history. Peak stress intensities were calculated from results per stress difference procedure in Section III, Appendix XIII-2400. Once alternating stress intensity is known, the next step calculated the stress relaxation history along the elastic follow-up. This step used the ISCCs with secondary creep rates only. The secondary creep rate equations of Class A materials per HBB-T-1800 were used. Creep damage fractions were calculated incrementally from stress history following Equation 1. Allowable time durations were calculated from the Class A minimum stress to rupture tables provided in HBB-I-14. The strain value at the end of dwell time is the enhanced strain range which incorporates strain increment due to elastic follow-up. The enhanced strain range was used to calculate design allowable cycles by using the Class

A fatigue life design curves in HBB-T-1420. The creep and fatigue damage fractions accumulated in one cycle were used to calculate the maximum allowable design cycle. For details of the numerical formulation for creep damage calculations and enhanced strain range determination with elastic follow-up, readers are recommended to review the previous report [3].

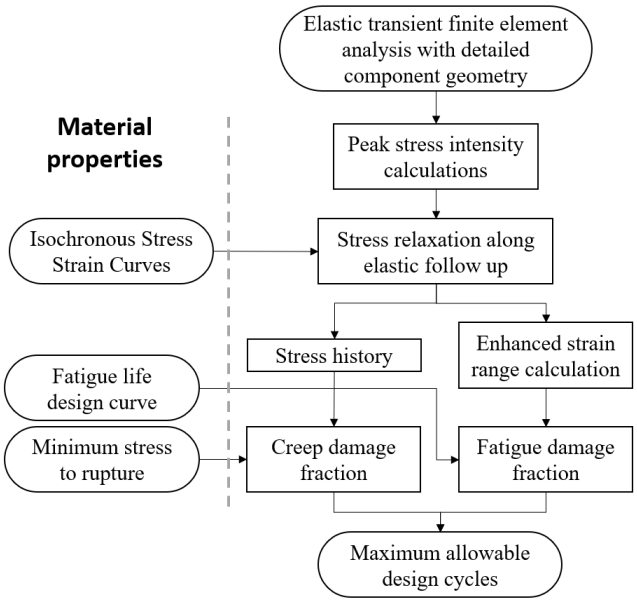

FIGURE 4: Flow chart of the creep-fatigue damage evaluation methodology per Class B rules.

The maximum allowable design cycle N_{max} is maximum attainable cycle achieved by component for a selected load cycle, where creep and fatigue damage fractions satisfy the creep-fatigue damage envelope. The N_{max} was used as a basis to evaluate the conservatism of proposed rules. If N_{max} calculated from Class B is lower compared to the failure cycles from experiments, Class B rules are conservative compared to test failure data. The N_{max} for the creep-fatigue damage intersection point of (0.2,0.2) is calculated per Equation 2.

$$\text{if } dD_c \geq dD_f, \quad N_{max} = \frac{1}{dD_c + 4dD_f}$$
$$\text{if } dD_c < dD_f, \quad N_{max} = \frac{1}{4dD_c + dD_f} \qquad (2)$$

Where dD_c and dD_f in equations above are creep and fatigue damage fractions accumulated in one cycle. The background document report [5] describes the detailed calculation.

The following discussion is separated into two categories. The first category evaluates the proposed Class B rules against failure cycles obtained from a set of cyclic experiments on standard ASTM specimens and scaled components. The second category used example problems to evaluate proposed rules against Class A elastic analysis methodology per ASME BPVC Section III, Division 5, HBB-T.

3.1 Comparison Against Test Failure Data

This subsection compares Class B results against test failure data through four different types of tests. The following discussion presents the test details and comparison of test failure cycles against the maximum allowable design cycles.

3.1.1 Single-Bar Simplified Model Test (SBSMT)

The Single-Bar Simplified Model Test (SBSMT) concept and implementation have been under extensive development as discussed in [6]. It is a test procedure that allows the generation of cyclic failure test data from key-feature test article but using standard ASTM cyclic specimens. Recent results [7] generated using the software controlled SBSMT concept for A617 material at 950℃ with a hold time of 10 minutes at tensile peak are shown in Table 1. These test results were used to evaluate the proposed Class B rules.

TABLE 1: Comparison of Class B results against test results for SBSMT.

Experimental data [7]			**Class B**		
q	$\Delta\varepsilon(\%)$	N_f	q	$\Delta\varepsilon(\%)$	N_{max}
3	0.22	4522	2	0.28	28

The default elastic follow-up of two yielded a conservative estimation of maximum allowable design cycles. The stress relaxation estimated from ISSCs with q = 2 is conservative compared to actual stress relaxation observed in experiment with q = 3 for first and for 400th cycle, as shown in Figure 5. This comparison suggests the stress relaxation equations with q = 2 bounds the stress relaxation histories observed in experiment. Therefore, the proposed creep damage evaluation approach bounds the creep damage fraction calculations. The enhanced strain range calculation gives a conservative estimate compared to the strain range in the SBSMT experiment, giving conservative fatigue damage fractions. The proposed creep-fatigue evaluation procedure yields a conservative estimate of the design life when compared against the failure cycles observed in SBSMT.

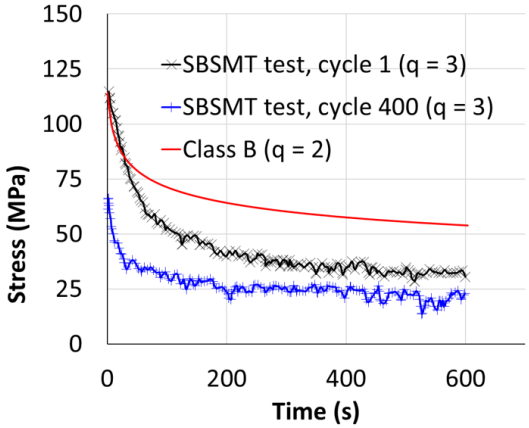

FIGURE 5: Comparison of stress relaxation profile from SBSMT test with q = 3 against ISSCs with q = 2.

3.1.2 Multiaxial Isothermal Tubes

Multiaxial isothermal tube experiments conducted by Majumdar [8] on SS316H straight-gauge geometry tubes were selected. These tubes were pressurized to 7.58 MPa at 593℃ and subjected to strain-controlled cyclic end displacements resulting in a strain range of 0.5%. The strain was held constant for one minute at peak strain, which resulted in an elastic follow-up value of one. The Class A elastic rules were applied to determine the maximum allowable design cycles. Table 2 presents the comparison of failure cycles from the test against the design cycles from Class A elastic rules and proposed Class B methodology.

TABLE 2: Comparison of Class B results against test results for multiaxial isothermal tubes.

Experimental data [8]			**Class A elastic**		**Class B (q=2)**	
q	$\Delta\varepsilon(\%)$	N_f	$\Delta\varepsilon(\%)$	N_{max}	$\Delta\varepsilon(\%)$	N_{max}
1	0.5	3821	0.543	463	0.89	128

Class B methodology with elastic follow-up of two conservatively bounds the design cycles when compared against the test failure cycle. The strain range calculated from Class B includes the additional strain accumulation during stress relaxation with q = 2. Therefore, Class B strain range is higher compared to the Class A strain range. Stress relaxation from the Class B approach gives higher stress intensities compared to the Class A stress relaxation approach, which result in larger creep damage accumulation. These reasons result in the lower design cycle estimation from Class B compared to Class A elastic methodology.

3.1.3 Pressurized Single-Bar Simplified Model Test (pSBSMT)

A series of cyclic tests has been conducted on tube-like SBSMT to study the influence of primary stress on the creep-fatigue life of A617 [9,10]. Experiment data obtained from the tube-like SBSMT test specimens fabricated with A617 material was selected [10]. The schematic figure of the pressurized SBSMT specimen is shown in Figure 6. These specimens were subjected to internal pressure at 950℃ and cyclic strain-controlled axial displacement load with pre-determined elastic follow-up values. The displacement load application used hardware-controlled strain cycles. A set of load parameters were selected to cover different ranges of pressures, strain ranges, and elastic follow-up values. These load cases were used, and maximum design cycles were calculated from the Class B approach, as shown in Table 3.

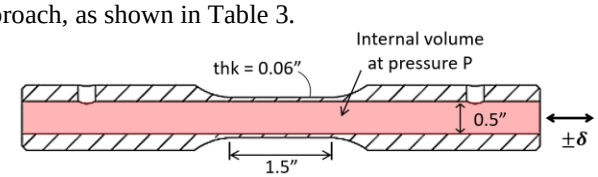

FIGURE 6: Sketch of the pressurized single-bar simplified model test sample showing dimensions and geometric details. All dimensions are in inches.

TABLE 3: Comparison of Class B results against test results for pressurized SBSMT tested at 950℃.

Experimental data [10]					**Class B N_{max} with q=2**
Test name	P (MPa)	q	$\Delta\varepsilon$ (%)	N_f	
SBAP4	0.01	6.10	0.18	3641	43
SBAP5	1.03	3.40	0.53	201	11
SBAP6	0.01	3.53	0.53	347	11
SBAP9	1.03	1.96	0.28	996	85
SBAP7	0.01	2.02	0.25	3224	85

The maximum design cycles with q = 2 bounds all test failure cycles for all cases. The Class B stress relaxation profile with q = 2 is compared to actual stress relaxation profile for first and 10th cycle, as shown in Figure 7. Despite using q = 2, the stress relaxation profile from Class B bounds the stresses observed in experiments with elastic follow-up of 6.1. This comparison suggests conservative creep damage calculation compared to test data and justifies the use of elastic follow-up value of two as a base line. The Class B creep-fatigue calculations were governed by creep damage fractions. Therefore, the Class B approach is conservative compared to the test failure cycles. This observation is consistent with SBSMT test results.

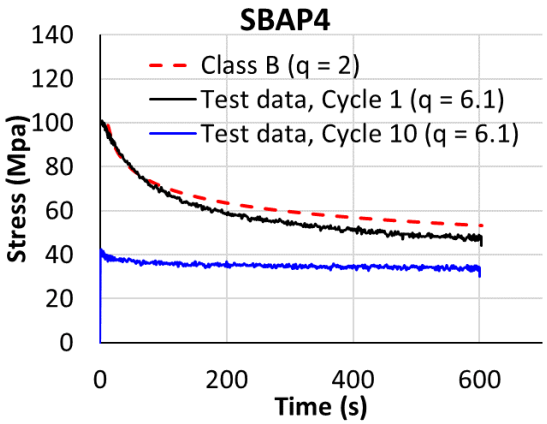

FIGURE 7: Stress and strain history using isochronous stress-strain curve relaxation intercepts.

3.1.4 Pressurized Simplified Model Test (pSMT)

The pSMT test specimen was developed and tested to capture the realistic component behavior [11-13]. The test procedure applies the strain range and pre-determined elastic follow-up. The schematic figure of the pSMT test specimen and the adopted displacement load profile is shown in Figure 8. The test specimen was internally pressurized at elevated temperature and subjected to cyclic end displacement measured over 5-in. gauge length (δ) with dwell. These load cycles with pSMT geometry capture the component-like response from the specimen. Six load cases were selected, as shown in Table 4. One load case has dwell time at compressive and tensile peak displacement.

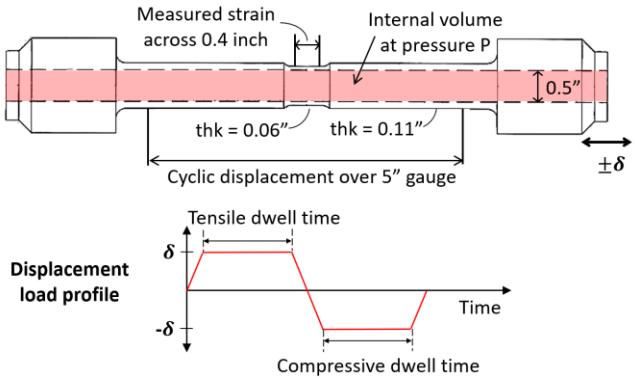

FIGURE 8: Sketch of the pressurized isothermal SMT test specimen geometry and displacement profile applied on the specimen end.

TABLE 4: Load case parameters of pSMT tests selected to evaluate proposed Class B methodology.

Load case	T (°C)	δ (mm)	Dwell time (sec)		P (MPa)
			Tensile	Compressive	
P01	950	0.1143	600	0	0.01
P05	950	0.1143	600	600	0.01
P02	950	0.1143	600	0	1.38
P12	950	0.0635	600	0	0.01
P14	850	0.0762	600	0	2.76
P15	850	0.0762	600	0	0.14

The pSMT geometry was modeled with an axisymmetric quarter model. The Class B calculations were performed and the N_{max} were compared against test failure cycles. For comparison purposes, Class A elastic analysis was performed, and maximum allowable design cycles were calculated. The maximum design cycles from Class B rules were consistently conservative by order of magnitude compared to the test failure cycles, as shown in Table 5. This comparison validates the conservatism in the proposed creep-fatigue damage calculations in the proposed Class B rules. Note that maximum design cycles from Class A are lower compared to Class B design cycles.

TABLE 5: Comparison of Class B results against test results and Class A elastic rules for pressurized SMT.

Load case	Test data [12]		Maximum design cycles	
	q	Failure cycles	Class A elastic	Class B
P01	3.8	220	0	12
P05	3.5	320	0	10
P02	3.8	220	0	12
P12	4.1	1360	3	39
P14	3.5	3440	5	142
P15	3.5	3460	6	142

3.2 Comparison Against Class A Elastic Methodology

This subsection will compare Class B against Class A elastic design rules for two example problems. A Bree problem with a wide set of load parameters and two materials was selected to conduct a parametric study. The second example problem is a flat head vessel with stress concentration factor.

3.2.1 Bree Problem with Simple Load Cycle

A standard Bree problem is a thin pipe under pressure with a temperature gradient across thickness. Conceptually, the Bree problem is comparable to multiaxial tube tests, with an addition of temperature gradient across thickness. The schematic diagram of the Bree problem is shown in Figure 9. The top and bottom nodes were constrained such that no shear deformation is allowed in the component. The temperature distribution on the internal diameter (ID) is presented in red. A linear temperature distribution is assumed across thickness, and temperature gradient of dT is maintained during dwell time. The internal radius is 1000 mm, and the thickness is 20 mm.

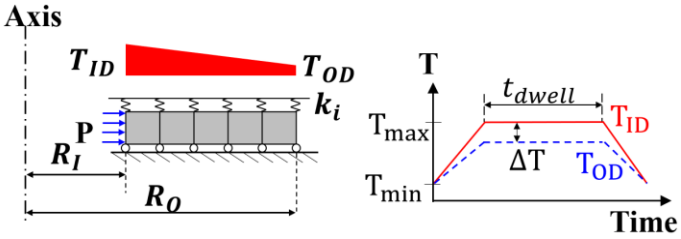

FIGURE 9: Schematic figure of the Bree problem and selected temperature profile.

A parametric study was conducted through a wider range of load parameters. The following key load parameters were selected: Maximum temperature (T_{max}), temperature gradient during dwell time (ΔT), and internal pressure (P). These load parameters were selected for 316H and A617 material to study the conservatism in the proposed Class B rules for different materials. Tables 6 and 7 summarize the load parameters selected for 316H and A617, respectively. Hold time for all load cases is 1000 hours.

TABLE 6: Bree problem load parameters for 316H material.

Load Case	T_{max} (°C)	P (MPa)	ΔT (°C)	Load Case	T_{max} (°C)	P (MPa)	ΔT (°C)
1	700	0	9.9	**10**	600	0	9.9
2			19.8	**11**			19.8
3			49.4	**12**			49.4
4		0.11	9.9	**13**		0.11	9.9
5			19.8	**14**			19.8
6			49.4	**15**			49.4
7		0.23	9.9	**16**		0.23	9.9
8			19.8	**17**			19.8
9			49.4	**18**			49.4

TABLE 7: Bree problem load parameters for A617 material.

Load Case	T_{max} (℃)	P (MPa)	ΔT (℃)	Load Case	T_{max} (℃)	P (MPa)	ΔT (℃)
41	900	0	12.1	**50**	800	0	12.1
42			24.2	**51**			24.2
43			60.5	**52**			60.5
44		0.13	12.1	**53**		0.11	12.1
45			24.2	**54**			24.2
46			60.5	**55**			60.5
47		0.26	12.1	**56**		0.23	12.1
48			24.2	**57**			24.2
49			60.5	**58**			60.5

The maximum allowable design cycles were calculated per proposed Class B methodology and following Class A elastic analysis procedure. A conservativeness ratio (CR) is calculated by dividing the N_{max} obtained from Class B by N_{max} calculated from Class A elastic rules. CR smaller than one suggests the proposed rules are conservative compared to the Class A elastic methodology. The CR of different load cases for 316H and A617 are presented in Figure 10a and 10b, respectively.

For 316H material, the maximum allowable design cycles from Class B are smaller compared to Class A cycles in general. Class B uses secondary creep rate equations only, which results in slower stress relaxation compared to Class A procedure. Creep damage calculation in Class B also has an explicitly defined elastic follow-up, which increases the creep damage fraction. Thus, the total creep damage from Class B is higher compared to the Class A procedure. In 316H at 600℃, primary creep has a significant influence. Not using primary creep at this temperature results in a slower stress relaxation, which yields more creep damage fractions per cycle and lower design life. This is observed in load case 10 to 18. Note that load Cases 12, 15, and 18 have the highest conservatism. These load cases have high thermal stresses that results in a larger stress intensity and the difference in stress relaxation from Class B and Class A is significant for these cases. For A617 material, Class A ISSCs have secondary creep rates that are identical to Class B ISSCs. Unlike Class B, Class A creep damage procedure uses stress amplification factor. Therefore, for load cases with a maximum temperature of 800℃, the Class A elastic analysis approach results in more conservative design cycles compared to the Class B. Although this affect is clearly observed at 800℃, other load cases have this effect in small amounts but generally is masked by the elastic follow-up.

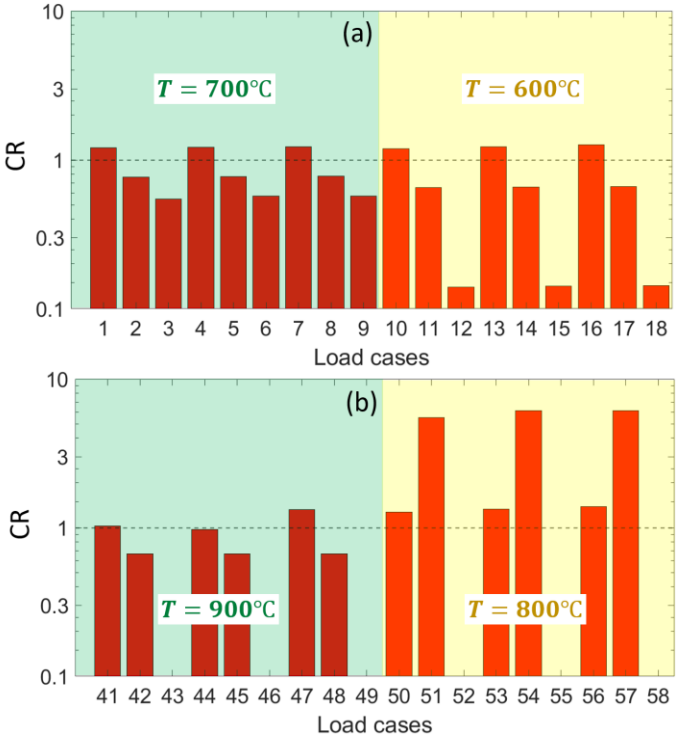

FIGURE 10: Ratio of maximum allowable design cycles calculated from Class B and Class A elastic approach for (a) 316H, and (b) A617 material.

3.2.2 Flat Head Vessel with Simple Load Cycle

A flat head vessel geometry is selected for 316H material, as shown in Figure 11. The knuckle is modeled with a smooth corner radius of 6.35 mm. The stress concentration ratio at this knuckle was 1.46. Internal dimensions were pressurized to 0.1 MPa. The temperature profile ID is applied to the internal dimensions and outer diameter (OD) is applied to the external dimensions. A linear temperature gradient of 20℃ is maintained during the dwell time. A set of dwell times were selected by keeping all other load parameters the same.

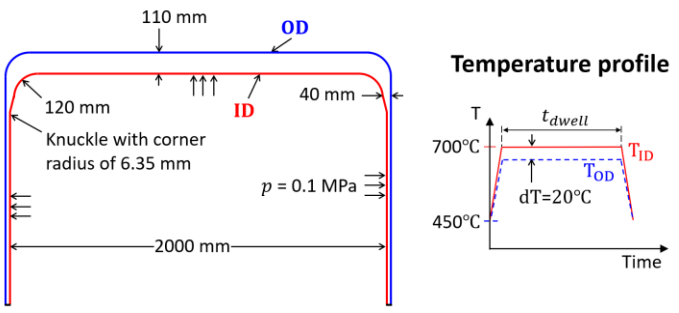

FIGURE 11: Flat head vessel component geometry and selected temperature profile.

Table 8 presents the maximum allowable design cycles from Class B and Class A methodologies. As noted before, Class A ISSCs for 316H uses primary and secondary creep rates, which

results in faster stress relaxation compared to Class B. The slower stress relaxation indicates more creep damage per cycle resulting in a conservative estimate of design life.

TABLE 8: Comparison of maximum allowable design cycles calculated from Class A elastic and Class B methodology.

ID	t_{dwell} (hr)	Class A N_{max}	N_{max} Class B with $q = 2$
1	10	312	35
2	30	127	23
3	100	47	15
4	300	18	10
5	1000	6	6
6	3000	2	3
7	10000	0	1

4. DISCUSSIONS

The maximum design cycles compared against the test failure cycles supported the use of elastic follow-up of two as a baseline value. The Class B creep-fatigue evaluation procedure is conservative compared to test failure cycles from experiments conducted on SBSMT, multiaxial tubes, pSBSMT, and pSMT test geometries. The pSBSMT and pSMT tests explicitly captured the elastic follow-up influence. Therefore, comparisons of maximum allowable cycles from the Class B creep-fatigue assessment are critical for pSBSMT and pSMT. Proposed Class B creep-fatigue methodology is conservative for pSBSMT and pSMT. The stress relaxation history calculated from creep rates in Class B ISSCs are conservative compared to the stress relaxation recorded in tests. The enhanced strain range per Class B procedure is consistently conservative due to explicit definition of elastic follow-up compared to strain ranges in experiments.

The following are key differences between the Class B DBA rules and the Class A elastic analysis procedure:

1. **ISSCs**: For the A617 tests, stress relaxation with q = 2 bounds the response of material with q = 6.1. ISSCs equations estimate slower stress relaxation compared to the stress relaxation observed in tests. Hence, proposed rules are conservative compared to the test data. Class A uses primary and secondary creep rates except for A617. Class B uses only secondary creep rates in ISSCs, which results in slower stress relaxation compared to Class A ISSCs with primary and secondary creep rates. The slower stress relaxation leads to higher creep damage fraction as observed for 316H material in the Bree problem and flat head vessel. Therefore, the Class B approach yields implicitly conservative estimates of design cycles compared to Class A approach, except for A617.
2. **An elastic follow-up**: Unlike Class A procedure, Class B uses explicit definition of the elastic follow-up while calculating creep and fatigue damage fractions. The proposed procedure links creep and fatigue damage calculations as both are calculated from the stress-strain relaxation information obtained from ISSCs along the elastic follow-up. The Class A elastic analysis does not use explicit elastic follow-up to calculate the stress relaxations and strain range calculations. Class B always results in a larger strain range compared to Class A elastic methodology and the fatigue damage is always conservative.
3. **Stress amplification factor**: The proposed Class B procedure does not use stress amplification factor K' while calculating the creep damage. The Class A elastic analysis approach uses K' of 0.9 for 316H and A617 materials, respectively. The stress amplification factor introduces conservativeness in the Class A design procedure. Influence of this factor is observed in the Bree problem with A617 at 800℃, where design cycles from the Class A elastic approach are lower compared to the Class B methodology.
4. **Creep-fatigue damage envelope**: The Class B procedure intends to use a material independent creep-fatigue envelope with (0.2, 0.2) intersection points. The maximum allowable cycles using this damage envelope gave conservative estimates when compared against the test failure cycles from all experiments. Class A procedure has explicit definitions of creep-fatigue damage envelopes for each material. The damage intersection points for 316H and A617 in Class A procedure are (0.3, 0.3) and (0.1, 0.1), respectively. Despite using the material independent creep-fatigue damage envelope, the maximum allowable design cycles from Class B are reasonably comparable to the maximum design cycles calculated from Class A elastic analysis.

As discussed above, the use of only secondary creep rates for the ISSCs leads to conservative creep damage estimates. Very little information is available on primary creep rates for the Class B materials. One could argue the use of primary creep rates is an important step; however, imposing primary creep rate for Class B materials poses additional data requirements. The goal is to minimize the material data demand to accelerate the acceptance and qualification of materials for Class B applications. At this point, using only secondary creep rates and associated conservatism is adopted. A potential solution is to approximate the primary creep rate for these candidate Class B materials from the behavior of similar materials or logical inferences thereof and assess the impact and credibility of the results. This avenue will be explored in the future.

The enhanced strain range calculations adopted in Class B are conservative compared to the Class A elastic analysis methodology. Therefore, Class B consistently estimates conservative design cycle for fatigue damage governed load cases compared to the Class A elastic method. The selection of the enhanced strain range will be revisited to assess this conservatism.

5. CONCLUSION

This paper proposes new DBA rules for Class B components and evaluates the creep-fatigue damage assessment approach through experimental results and example problems. An order of magnitude of conservatism is observed between maximum design cycles from Class B and failure cycles from SBSMT, multiaxial tubes, pSBSMT, and pSMT experiments. This observation supports the use of general elastic follow-up value of two and use of intersection point (0.2,0.2) for the creep-fatigue damage envelope. Two sets of example problems were selected with a wide set of load cycles, and proposed Class B rules were evaluated against the Class A elastic analysis procedure per HBB Section III, Division 5. This study also showed that using only secondary creep rates results in a conservative design life estimation compared to the Class A elastic analysis approach. Additional conservatism in the creep and fatigue damage fractions will be addressed in the future work.

ACKNOWLEDGEMENTS

The research was sponsored by the U.S. Department of Energy, Office of Nuclear Energy, under Contract No. DE-AC05-00OR22725 with Oak Ridge National Laboratory (ORNL), managed and operated by UT-Battelle, LLC, and under Contract No. DE-AC07-05ID14517 with Idaho National Laboratory (INL), managed and operated by Battelle Energy Alliance, LLC. Programmatic direction was provided by the Office of Nuclear Reactor Deployment of the Office of Nuclear Energy.

COPYRIGHT NOTICE

REFERENCES

[1] American Society of Mechanical Engineers (ASME) International. 2023. “Section III, Rules for Construction of Nuclear Facility Components, Division 5, High Temperature Reactors.” in ASME Boiler and Pressure Vessel Code: An International Code. New York, NY.

[2] American Society of Mechanical Engineers (ASME) International. 2023. “Section II, Materials, Part D, Properties.” in ASME Boiler and Pressure Vessel Code: An International Code. New York, NY.

[3] Sham, T.L., Wang, Y. and Mahajan, H.P., “Initial Development of Variable Design Lifetimes and Creep-Fatigue Evaluations for ASME Section III, Division 5, Class B Code Rules.” INL/RPT-22-69139, Idaho National Laboratory (INL), Idaho Falls, ID, 2022.

[4] Jetter, Robert I. "An Alternate Approach to Evaluation of Creep-Fatigue Damage for High Temperature Structural Design Criteria." ASME-PUBLICATIONS-PVP 365 (1998): 199-206.

[5] Mahajan, H.P., Jetter, R.I.., Wang, Y. and Sham, T.L. “FY-23 Status Report on the Development of New ASME Section III, Division 5 Class B Rules” INL/RPT-23-74748, Idaho National Laboratory (INL), Idaho Falls, ID, 2023.

[6] Wang, Y., Jetter R.I., Messner M.C. and Sham T.L., “Development of Simplified Model Test Methods for Creep-Fatigue Evaluation”, Proceedings of the ASME 2019 Pressure Vessels and Piping Conference, PVP2019-93648, July 2019.

[7] Mahajan, H. P. and McMurtrey, M. D. “Single-Bar SMT Creep-Fatigue Testing on Alloy 617 with Software Controls on Elastic Follow-Up Feedback in Support of New Creep-Fatigue Design Methodology.” INL/RPT-22-68896, Idaho National Laboratory (INL), Idaho Falls, ID, 2022.

[8] Majumdar, S. “Biaxial Creep-Fatigue Behavior of Type 316H Stainless Steel Tube.” No. ANL-79-33. Argonne National Laboratory (ANL), Argonne, IL, 1979.

[9] Wang Y., Hou, P., Jetter R.I. and Sham T.L., “Evaluation of Primary-load Effects on Creep-Fatigue Life of Alloy 617 Using Simplified Model Test Method”, Proceedings of the ASME 2021 Pressure Vessels and Piping Conference, PVP2021-61658, July 2021.

[10] Wang, Y., Hou, P., Jetter, R.I. and Sham, T.L., “Report on FY2020 Test Results in Support of the Development of EPP Plus SMT Design Method.” ORNL/TM-2020/1620, Oak Ridge National Laboratory (ORNL), Oak Ridge, TN, 2022.

[11] Wang Y., Jetter R.I. and Sham T.L., “Pressurized Creep-Fatigue Testing of Alloy 617 Using Simplified Model Test Method”, Proceedings of the ASME 2017 Pressure Vessels and Piping Conference, PVP2017-65457, July 2017.

[12] Wang, Y., Jetter, R.I., Messner, M.C. and Sham, T. L., “Report on FY19 Testing in Support of Integrated EPP-SMT Design Methods Development.” ORNL/TM-2019/1224, Oak Ridge National Laboratory (ORNL), Oak Ridge, TN, 2019.

[13] Wang Y., Jetter R. I. and Sham T.L., “Effect of Internal Pressurization on the Creep-Fatigue Performance of Alloy 617 Based on Simplified Model Test Method”, PVP2019-93650, July 2019.

